

ANALYSIS OF MITOSIS DETECTION TECHNIQUES FOR
BREAST HISTOPATHOLOGICAL IMAGES

A Project Report

Submitted by

Mr. ABDUL RAHIM SHIHABUDDIN

REG NO : TKM20MEAI01

SEMESTER : IV

In partial fulfillment for the award of the degree of

MASTER OF TECHNOLOGY

IN

Mechanical Engineering (Artificial Intelligence)

Under the guidance of

Dr. SABEENA BEEVI K



Thangal Kunju Musaliar College of Engineering
Kerala

JULY 2022

DECLARATION

I undersigned hereby declare that the project report "**Analysis of mitosis detection techniques for breast histopathological images**", submitted for partial fulfillment of the requirements for the award of degree of Master of Technology of the APJ Abdul Kalam Technological University, Kerala is a bonafide work done by me under supervision of **Dr.Sabeena Beevi K**. This submission represents my ideas in my own words and where ideas or words of others have been included, I have adequately and accurately cited and referenced the original sources. I also declare that I have adhered to ethics of academic honesty and integrity and have not misrepresented or fabricated any data or idea or fact or source in my submission. I understand that any violation of the above will be a cause for disciplinary action by the institute and/or the University and can also evoke penal action from the sources which have thus not been properly cited or from whom proper permission has not been obtained. This report has not been previously formed the basis for the award of any degree, diploma or similar title of any other University.

Place: Kollam

Date:

ABDUL RAHIM SHIHABUDDIN

Thangal Kunju Musaliar College of Engineering
Centre for Artificial Intelligence



C E R T I F I C A T E

This is to certify that, this report titled ***ANALYSIS OF MITOSIS DETECTION TECHNIQUES FOR BREAST HISTOPATHOLOGICAL IMAGES*** is a bonafide record of the **Project** presented by **ABDUL RAHIM SHIHABUDDIN(TKM20MEAI01)**, under our guidance and supervision, in partial fulfillment of the requirements for the award of the degree, **M.Tech in Mechanical Engineering (Artificial Intelligence)** in **APJ Abdul Kalam Technological University** .

Internal Supervisor

Project Coordinator

Head of the Department

Dr. Sabeena Beevi K
Assoc. Professor & Head
Dept. of EEE,
TKMCE

Prof. Sumod Sundar
Assistant Professor
Centre for Artificial Intelligence,
TKMCE

Dr. Imthias Ahamed
Professor & Head
Centre for Artificial Intelligence,
TKMCE

Internal Examiner

External Examiner

ACKNOWLEDGEMENT

A successful project is a fruitful culmination of efforts by many people, some directly involved and some others indirectly, by providing support and encouragement. Firstly I would like to thank the almighty for giving me the wisdom and grace for making my project a successful one. I thank him for steering me to the shore of fulfillment under his protective wings.

I express my sincere gratitude to **Dr. T A Shahul Hameed**, Principal of TKMCE, for providing me the opportunity to work on this project . I would like to thank **Dr. Imthias Ahamed**, Professor and Head of the Department, Centre for Artificial Intelligence, TKMCE, for his constant support and encouragement throughout the project work.

I am immensely indebted to my guide **Dr. Sabeena Beevi K** , Associate Professor and Head of the Department, Department of Electrical and Electronics Engineering, for her constructive guidance and advice.I would like to express my heartfelt thanks to our project coordinator **Prof. Sumod Sundar**, Assistant Professor, Centre for Artificial Intelligence, TKMCE, for his expert guidance and cooperation. With a profound sense of gratitude, I would like to thank **Dr.Santhi Natarajan**, Honorary Professor, for her immense encouragement. I also extend my thanks to **Prof.Chinnu Jacob**,Assistant Professor, Centre for Artificial Intelligence, TKMCE, and other staff members of the Centre for AI, TKMCE, who has encouraged me throughout this work.

I also express my thanks to my loving parents, sister and friends, for their support and encouragement in the successful completion of this project work.

ABDUL RAHIM SHIHABUDDIN

Abstract

The number of mitotic cells is an important metric in the diagnosis of breast cancer. It gives the extent to which the tumor has spread, which has further implications in predicting cancer's aggressiveness. Mitosis counting is a laborious and complex process done manually by a pathologist by analyzing Hematoxylin and Eosin (H&E) stained biopsy slices under a microscope. Detection of mitosis in H&E stained slices is difficult due to insufficient datasets and the similarity between mitotic and non-mitotic cells. The advent of computer-aided mitosis detection methods made the whole process far easier by helping in screening, identifying and labeling mitotic cells. Traditional detection methods relied on image processing techniques in which image features are distinguished using handcrafted features. The development and application of neural networks have also been investigated in the mitosis detection process due to their ability to extract features automatically. This project investigates mitosis detection as both a classification problem and an object detection problem. The mitosis classification problem employed a multiCNN framework for feature extraction and used machine learning techniques for classification. Tissue level detection of mitosis was also investigated using pre-trained Faster R-CNN by taking raw images as in medical perspective. The experiments were carried out on two publicly available datasets, MITOS-ATYPIA-14 dataset and the latest TUPAC16 dataset and the results were compared with other methods in the literature.

Contents

1	Introduction	1
1.0.1	Objective	2
2	Related Works	3
3	Datasets	6
3.1	MITOS-ATYPIA-14 Dataset	6
3.2	TUPAC16 Dataset	7
4	Methodology	8
4.1	Analysis of Mitosis detection as a classification problem	8
4.1.1	Pre-processing	9
4.1.2	Cell segmentation and localisation	11
4.1.3	Feature Extraction using MultiCNN framework of Pre-trained CNNs	12
4.1.4	Concatenation of features to form multiCNN	14
4.1.5	Feature Reduction	15
4.1.6	Classification of cells	15
4.1.7	Training	16
4.1.8	Hyperparameter Tuning	16
4.1.9	Performance Measures	17
4.2	Analysis of Mitosis detection as an object detection problem	18
4.2.1	Dataset Preparation	19
4.2.2	Initial Tissue Level Detection using a pre-trained Faster R-CNN . . .	20
4.2.3	Cell Level Detection using MultiCNN framework	22
4.2.4	Feature Reduction and Classification of cells	22
4.2.5	Performance Measures	22
5	Results and Discussions	23
5.1	Analysis of Mitosis detection as a classification problem	23
5.1.1	Datasets considered	23
5.1.2	Performance comparison of dimensionality reduction methods	23
5.1.3	Performance comparison of multiCNN composed of 6 pre-trained CNNs with different classifiers	23
5.1.4	Results of pre-trained multi-CNN with different combinations of net- works on MITOS-ATYPIA-14 dataset	24
5.1.5	Classification Results obtained on TUPAC16 dataset	27

5.1.6	Results of proposed method with the other methodologies in the literature	29
5.2	Analysis of mitosis detection as an object detection problem	29
5.2.1	Detection of patches from the test images using Faster R-CNN	29
5.2.2	Performance comparison of multiCNN architecture with a single pre-trained CNN on MITOS-ATYPIA-14 dataset	29
5.2.3	Performance comparison of multiCNN composed of 5 pre-trained CNNs with different classifiers	32
6	Conclusion	33
	References	34

List of Figures

3.1	Sample Images from MITOS-ATYPIA-14 dataset	7
3.2	Sample Images from TUPAC16 dataset	7
4.1	Proposed framework for mitosis classification	9
4.2	Sample images from A03,A04, A05 folders of MITOS-ATYPIA-14 dataset .	11
4.3	Sample images from A03,A04, A05 folders of MITOS-ATYPIA-14 dataset after stain normalisation	11
4.4	Number of instances in each dataset	12
4.5	Proposed framework For Both Tissue and Cell Level Classification	18
4.6	Separating the images into 4 quadrants	19
4.7	For preparation of patches as training data for object detection, bounding boxes should be drawn around ROI. Labelme tool is used for this purpose. .	20
4.8	Labelme Tool for Bounding Box Preparation	20
4.9	Mitosis Detection using Faster R-CNN	21
5.1	ROC curve corresponding to multiCNN of 6 pre-trained CNNs' results ob- tained in MITOS-ATYPIA-14 dataset	26
5.2	ROC curve corresponding to multiCNN of 6 pre-trained CNNs' results ob- tained in TUPAC16 dataset	28
5.3	Mitosis Detection using Faster R-CNN	30
5.4	Detected objects which are cropped out from testing data	30
5.5	ROC curve corresponding to results obtained after cell level classification . .	32

List of Tables

2.1	Review of related recent works	5
3.1	Description of MITOS ATYPIA 14 dataset with Total Number of Images (TNI)	6
3.2	Description of TUPAC16 dataset with Total Number of Images (TNI)	7
5.1	Comparison of results obtained for multiCNN of 6 pre-trained CNNs using different dimensionality reduction methods with non-linear SVC as classifier	23
5.2	Comparison of results obtained for multiCNN of 6 pre-trained CNNs using different classifiers	24
5.3	Results of various multiCNN modelwith Non-Linear SVC as classifier	25
5.4	Confusion matrix corresponding to multiCNN of 6 pre-trained CNNs coupled with non-linear SVC on MITOS-ATYPIA-14 dataset	26
5.5	Results of concatenation of features from different pre-trained networks with Non-Linear SVC as classifier	27
5.6	Confusion matrix corresponding to multiCNN of 6 pre-trained CNNs coupled with non-linear SVC	28
5.7	Results of different deep learning based mitosis detection methods with proposed method	29
5.8	Results of concatenation of features from different pre-trained networks with Logistic Regression as classifier	31
5.9	Comparison of results obtained for multiCNN of 5 pre-trained CNNs using different classifiers	32

ABBREVIATIONS

AMIDA13	Assessment of Mitosis Detection Algorithms 2013
CNN	Convolutional Neural Network
FCL	Fully Connected Layer
FCN	Fully Convolutional Network
GLCM	Gray Level Co-occurrence Matrix
H&E	Hematoxylin and Eosin
HPF	High Power Field
LBP	Local Binary Pattern
MLE	Maximum Likelihood Estimation
PCA	Principal Component Analysis
RBF	Radial Basis Function
R-CNN	Region-Based Convolutional Neural Network
ROC	Receiver Operating Curve
ROI	Region Of Interest
RPN	Region Proposal Network
SVC	Support Vector Classifier
SVD	Singular Value Decomposition
SVM	Support Vector Machine
SSIM	Structural Similarity Index Metric
TUPAC16	Tumor Proliferation Assessment Challenge 16
VGG	Visual Geometry Group
XGBoost	eXtreme Gradient Boosting

Chapter 1

Introduction

Mitosis counting is one of the critical features that can accurately diagnose breast cancer and the patient's prognosis. Mitotic cells are primarily formed during cell division. These histopathological images are stained by Hematoxylin & Eosin (H&E) which can accentuate the components of cells and tissue and hence it is also used in breast cancer slices. Pathologists manually count mitosis in tumour tissue samples. During manual mitosis counting, a visual survey of whole slide images (WSI) would give an idea of where the highest mitotic activity occurs. There is a lack of equipment to help their process. The whole process is time consuming and complex.

Thus computer aided diagnosis is performed to achieve auxiliary diagnosis by means of medical image processing and computer analysis and improves the accuracy rate. Automated mitosis detection methods work by a model trained on annotated training data. The model can classify new histopathological slices as mitotic and non mitotic nuclei. Thus the automated detection methods can handle repetitive, tedious work when doctors work on treating the problem. However, the problem of automated mitosis detection methods is still complex due to following factors. First, there exist similarities between mitotic and non mitotic cells. Prophase, metaphase, anaphase, and telophase are different stages of mitosis with their own morphological characteristics. In the case of telophase, the nuclei is divided into two, but they are still counted as single cell which can result in misclassification. Second, many other objects (e.g., apoptotic cells, dense nuclei, lymphocytes) with the same morphology as mitotic cells can be present in HE dyed images which may lead to their misclassification as mitosis. Third, the density of mitoses in a single HPF is very low in comparison with other non-mitotic cells, making the detection very difficult due to class imbalance.

The application of deep learning models in the field of medical imaging severely lacks enough labeled data for effective training and thus transfer learning is adopted. Transfer learning refers to the process of transferring the weights of a pre-trained model to a new problem set on a different dataset. The idea is to transfer information from an already trained task to another task. To make changes to the current model, the network must be fine-tuned to the nature of the dataset. To tackle lack of datasets to train automated detection methods, datasets such as MITOS 2012, AMIDA-13, MITOS-ATYPIA-14 dataset, TUPAC16 datasets are generated from international competitions for mitosis detection analysis. These existing public datasets still differ from each other. Training on these datasets cannot guarantee the generalization capability of automated mitosis detection methods.

Within the deep learning approaches, the problem of mitosis detection have been formu-

lated as a classification problem or a segmentation problem or an object detection problem.

This work investigates the mitosis detection as both as a classification and an object detection problem. The analysis of mitosis detection as a classification problem investigates the performance of the multi CNN framework of pre-trained networks in automatic mitosis detection methods. A multi CNN framework composed of pre-trained CNN has never been employed in the study of mitosis detection. It is expected to improve the robustness of mitosis detection. The tissue samples from publicly available datasets such as MITOS-ATYPIA-14 and TUPAC16 datasets reveal stain variance due to adverse conditions, such as operator neglect, inadequate lighting, or HE staining depth in the process of separating histopathological slices. This requires stain normalization before segmenting the mitotic and non mitotic cells for classification and it is carried out by Reinhard normalization. As stated, the density of mitoses in a single HPF is very low compared to non mitotic cells which require data augmentation to avoid class imbalance. The proposed method extracts and combines generic low-level features and complex features from the localized cells by pretrained CNNs. The strength of different classifiers such as LinearSVC, Non-linear SVC, Logistic Regression, Random Forest , Adaboost, and XGBoost Classifiers are employed to deal with complex high dimensional features where the number of features are larger than the number of instances. Principal Component Analysis was used to reduce the dimensions of these features to better the performance of classifiers. The discriminant features from the pre-trained CNNs provide significant reduction in false positive rate and overcome the need for large labelled data.

The next analysis of mitosis detection is done by considering it as an object detection problem using pretrained Faster R-CNN and also addressing the problem on a cell level classification using multiCNN framework. Thus it addresses the problem on both tissue and cell level. The report is organized such that Section 2 presents relevant literature related to this work. Section 3 discusses the datasets used and Section 4 introduces the methodology and gives an overview of components used and Section 5 discusses experimental results, and the conclusions are drawn in Section 6.

1.0.1 Objective

1. To work on this mitosis detection as a classification problem by utilising a multiCNN framework for feature extraction and classification were done using machine learning classifiers.
2. To work on this mitosis detection as an object detection problem by utilising a pre-trained Faster R-CNN and employing cell level classification using multiCNN framework.

Chapter 2

Related Works

In this section, several studies of mitosis detection utilizing both machine learning and deep learning techniques are discussed.

Manual feature extraction was performed using image processing approaches that differentiate features manually. These constructed manual features are utilised to train the classifier to distinguish between mitotic and nonmitotic cells. Image features such as texture, first order and second order statistics are retrieved directly. The image are first sliced to narrow down on candidate regions, and then features are extracted from these candidate regions. Tashuk et.al employed 2D anisotropic diffusion and MLE to extract semantic information and LBP from images, which were then used to train an SVM classifier [1]. The study provided a mitotic cell detection method based on texture, SIFT, intensity, and morphological data extracted from images using multiple image channels. These features were so correlated resulting in poor classification [2]. Intensity features and morphological features from localized mitotic regions were extracted in [3] for mitosis detection and it gave an average F-score of 73 %. In another work, CLBP, GLCM features were extracted from localised regions and classified using a SVM classifier [4]. These regions were localised using Gamma-Gaussian mixture model. The work proposed an application of a set of features and an ensemble of cascade adaboosts on MITOS12 dataset gave a F-score of 58% [5] .

Due to its excellent automatic feature extraction and self-learning capabilities, deep learning based approaches are one of the most common types of algorithms used to address the challenge of recognising mitoses from histological images. Deep learning algorithms for mitosis detection were first reportedly used by D. Cireşan et al. [6]. A supervised Deep Neural Network (DNN), a convolutional neural network (CNN) with deep max-pooling layers, was used to detect mitosis. The network was built with five convolution layers and five maximum pooling layers, followed by two fully connected layers to identify mitosis. E. Zerhouni et al. used the vast residual network. The model is trained to identify each pixel and determine the likelihood of mitosis while filtering out noise. Shapes with minimal area were filtered out, leaving the centroid's remaining area as the detection result [7]. In the MICCAI TUPAC 2016 competition for mitosis detection, their technique came in second place. H. Chen et al. developed a coarse retrieval model based on two convolution neural networks cascaded together to locate candidate cells, which were then fed into a discrimination model to distinguish cells [8].

K. S. Beevi et al. suggested a multiclassifier system based on a deep belief network. The model was tested on a dataset from the mitosis competition. To create features for training

a classifier, the majority of these approaches relied on accurate nuclei segmentation [9]. Mitosis detection has also been a problem of object detection. Researchers have used R-CNN, Faster R-CNN, and Mask R-CNN as effective target detection approaches. Scratch CNNs were utilised for segmentation and detection in the majority of earlier mitotic detection studies, which could be time intensive. R-CNN architecture were modified with a pre-trained ResNet101 feature extraction network used large separable convolution to obtain a thin feature map to ensure better detection speed when ROI is obtained [10]. A multi stage model based on a faster R-CNN network and deep CNN was proposed to reduce false positive instances in the work of T. Mahmood [11]. M.Sebei et.al proposed a partial supervision framework called PartMitosis based on two parallel deep FCN was designed [12]. One FCN used weak labels for training, and the other FCN used strong labels for training and had a weight transfer function. The final detection is done by fusing the segmentation maps of each network. MaskMitosis, a framework specifically designed from Mask R-CNN for mitosis detection performs two problems: object detection and instance detection[13].

To tackle the time consumption to train the network models, the transfer learning method was utilized by K.Beevi et.al.[14]. Their paper explored the feasibility of using a pre-trained convolutional neural network for mitosis detection. The pre-trained CNN is used to isolate discriminant features from nuclei regions, and a random forest classifier is used to accurately predict each nuclei's class label. V. Dodbballapur et al.employed an application of deep learning methods with handcrafted features [15]. They employed a Mask R-CNN to generate masks of these histopathological images and then combine the mask with original image to generate manual features. These features are in turn concatenated to deep features extracted from Xception network and handcrafted features and input it into two fully connected layers for classification. N.Wahab, A.Khan, and colleagues employed pre-trained models to detect mitosis [16]. Mitosis is segregated using pre-trained CNNs in the first stage. The result is produced in the second stage using the hybrid CNN (HCNN). With an F-score of 0.713, fine-tuning-based Transfer Learning enhanced detection rate, shortened training time, and offered better startup weights.

To improve the accuracy and robustness of mitosis detection, this work proposes a multi CNN consisting of pretrained CNN architectures. After reading various pieces of literature, it has been found that a multi CNN framework composed of pre-trained CNN has never been employed in the problem of mitosis detection. We were inspired by the work of Bejoy et al. who developed a multi CNN framework for computer assisted detection of COVID images [17]. This work investigates the mitosis detection as both as a classification problem and an object detection problem using pretrained Faster R-CNN and also addressing the problem on a cell level classification using deep CNNs. The method is expected to address the problem on a tissue level and on a cell level. The advantages and disadvantages of some of the previous works are listed below:

The advantages and limitations of 4 recent related works are summarized in Table 2.1.

ANALYSIS OF MITOSIS DETECTION TECHNIQUES FOR BREAST HISTOPATHOLOGICAL IMAGES

Title	Technique used	Advantages	Disadvantages
Artificial Intelligence-Based Mitosis Detection in Breast Cancer Histopathology Images Using Faster R-CNN and Deep CNNs [2] - 2020	Faster R-CNN + Extraction of handcrafted features+ResNet50 and DenseNet201	Addressed the problem on tissue level and cell level. Less number of false positives	Datasets are insufficient to effectively train deep learning models
MaskMitosis: a deep learning framework for fully supervised, weakly supervised, and unsupervised mitosis detection in histopathology images	MaskMitosis-modified Mask R-CNN	Requires only one network to retrieve and classify mitosis candidates	Datasets are insufficient to effectively train deep learning models.
SmallMitosis: Small Size Mitotic Cells Detection in Breast Histopathology Images [18]	Multi-scale Region Proposal Model (MS-RCNN) + Atrous Fully Convolutional Network (A-FCN)	First time mitotic cell size oriented detection system is proposed. Reduces computational cost due to fully convolution layer in the end .Faster than Faster-RCNN detector.	Employs different networks for segmentation and classification.
A multi-phase deep CNN based mitosis detection framework for breast cancer histopathological images [19]	MP-MitDet	Good generalization ability with different datasets.	Learning capacity of different CNNs can be improved by combining feature spaces of diverse CNN architectures,

Table 2.1: Review of related recent works

Chapter 3

Datasets

There were serious lack of datasets for universal study of mitosis detection in breast cancer histopathology images. So in order to tackle the problem, mitosis competitions were held at international conferences for preparation of datasets. These competitions served as a resource They provide a unified evaluation standard for comparisons between different methods and for everyone’s discussion and communication by conducting experimental comparisons on the same dataset. Four publicly available datasets are generated for study- MITOS 12, AMIDA13 , MITOS-ATYPIA-14 , and TUPAC16 . Here in this work, MITOS-ATYPIA-14 and TUPAC 16 were taken.

3.1 MITOS-ATYPIA-14 Dataset

The MITOS-ATYPIA-14 grand challenge featured the ICPR 2014 or MITOS-ATYPIA-14 dataset. Mitosis detection and nuclear atypia assessment are both included in the dataset. HE was used to stain the pathological sections, and the Aperio Scanscope XT and Hamamatsu Nanozoomer 2.0-HT were used to scan them. Each image is 1539x 1376 pixels at 40 magnification, which is significantly smaller than the MITOS 2012 dataset. Only the centroid pixels of each mitosis were annotated by the pathologists. This dataset has significant variations in the dataset images due to its processing and acquisition conditions. The description of MITOS-ATYPIA-14 dataset with Total Number of Images(TNI) was shown in Table 3.1. Figure 3.1 shows the sample images from MITOS-ATYPIA-14 dataset.

Dataset Folder	A03	A04	A05	A07	A10
TNI	96	128	112	64	80

Dataset Folder	A11	A12	A14	A15	A17	A18
TNI	128	144	160	96	80	112

Table 3.1: Description of MITOS ATYPIA 14 dataset with Total Number of Images (TNI)

3.2 TUPAC16 Dataset

In 2016, the Tumor Proliferation Assessment Challenge proposed another annotated mitosis dataset that could be used by interested parties. These datasets contained a total of 73 cases from three different pathology centres. The first 23 cases' data were obtained from the AMIDA13 challenge. These images measure 2000 x 2000 pixels. The 50 newly added slices were HPF images scanned with a Leica SCN400 scanner, with each image measuring 5657 x 5657 pixels. This dataset is taken for cross experiment testing of the proposed method. The description of MITOS-ATYPIA-14 dataset with Total Number of Images(TNI) was shown in Table 3.2. Figure 3.2 shows the sample images from TUPAC16 dataset.

Dataset Folder	01	02	03	04	05	06	07	08	09	10	11	12	13
TNI	39	28	16	61	10	61	43	10	10	10	13	10	10

Dataset Folder	14	15	16	17	18	19	20	21	22	23	24-73
TNI	15	49	10	10	67	10	10	44	48	22	50

Table 3.2: Description of TUPAC16 dataset with Total Number of Images (TNI)

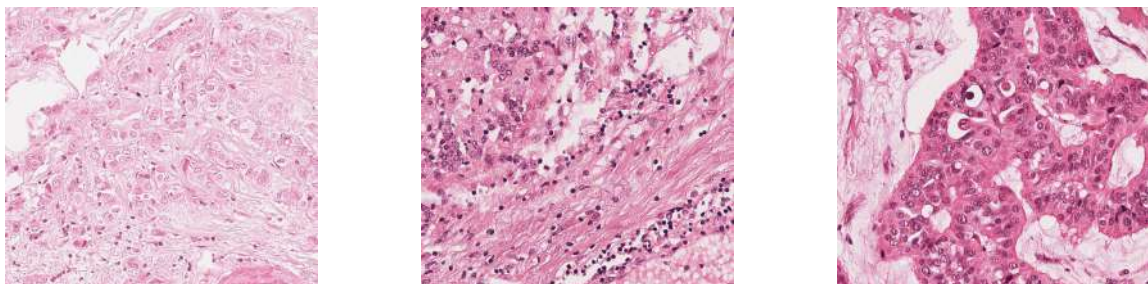


Figure 3.1: Sample Images from MITOS-ATYPIA-14 dataset

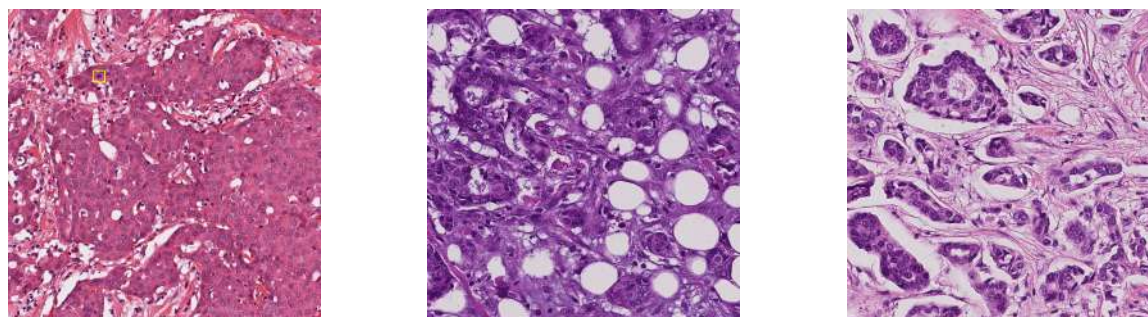


Figure 3.2: Sample Images from TUPAC16 dataset

Chapter 4

Methodology

4.1 Analysis of Mitosis detection as a classification problem

Here in this analysis, the mitosis detection was formulated as a classification problem with application of multi-CNN architecture for feature extraction. The proposed framework in this analysis was comprised of three steps such as :

1. Pre-processing including stain normalisation
2. Cell localisation
3. Feature Extraction using Pre-trained CNNs
4. Concatenation of extracted features to form different multiCNN
5. Feature Reduction
6. Classification of cells

In the first stage, the input images from the original dataset had undergone stain normalisation so the variance of staining in each image is minimised. These stain normalised images are subjected to undergo cell localisation so that mitotic and non-mitotic cells can be separated on the basis of its coordinates. These mitotic and non-mitotic cells obtained from both TUPAC16 and MITOS-ATYPIA-14 dataset constitute two training sets for classification problem. In stage 3, these training sets are used to undergo feature extraction using pre-trained CNNs. These features are concatenated in different combinations and passed through a dimensionality reduction method in stage 5. The proposed framework for mitosis classification is shown in Figure 4.1.

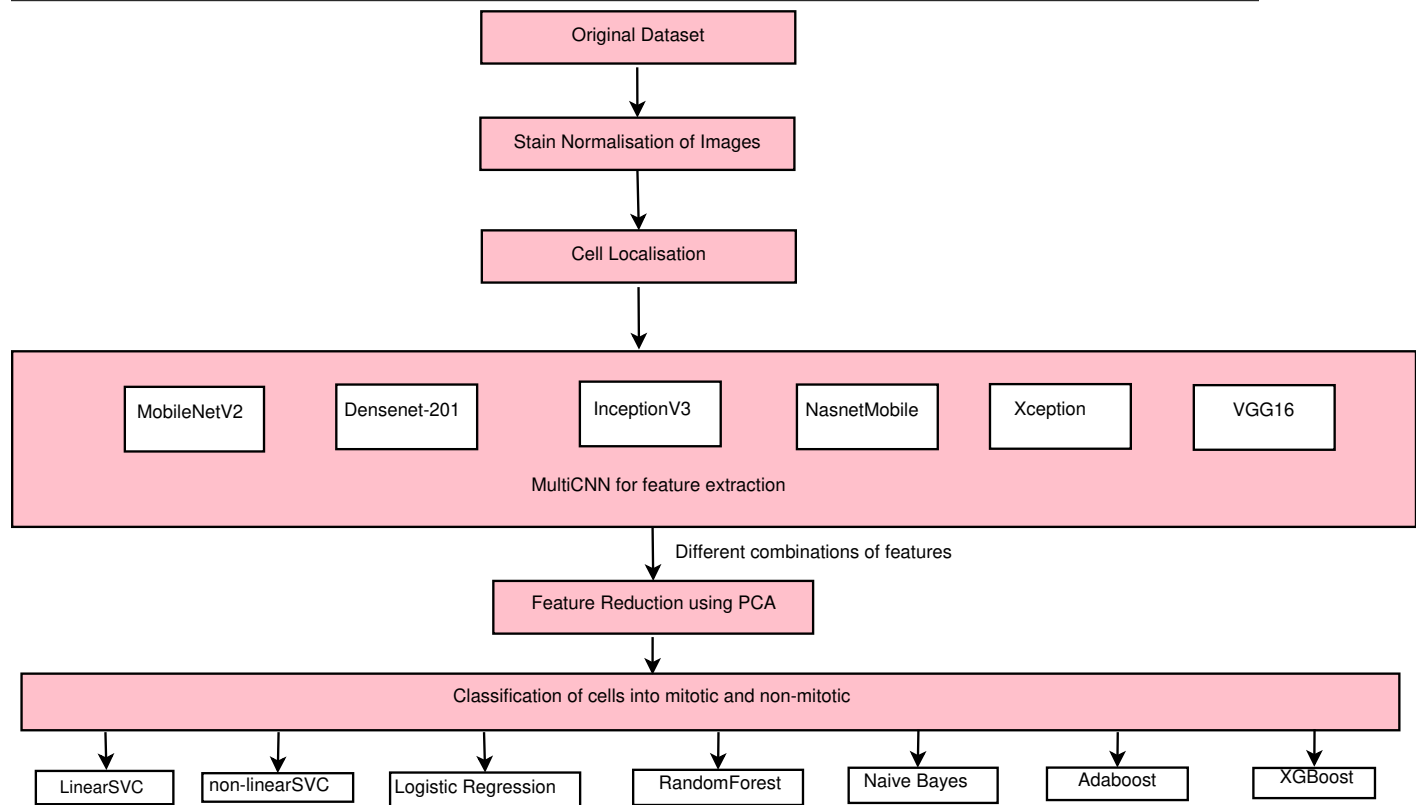


Figure 4.1: Proposed framework for mitosis classification

4.1.1 Pre-processing

Stain normalization

Tissue samples from the MITOS-ATYPIA-14 and TUPAC16 datasets reveal stain variance due to adverse conditions, such as operator neglect, inadequate lighting, or HE staining depth in the process of separating histopathological slices. These factors hamper the generalization of automatic image analysis method. Hence there is a need for standardizing the image before analysis by performing stain normalization which is achieved by removing the stains for visual enhancement. As a result, Reinhard normalisation , a stain normalization technique is performed . The colour distribution of an image that is under or over stained is mapped to that of a target image that has been well stained using Reinhard normalisation. This is achieved by executing a linear transformation in Lab colour space on each colour channel's mean and standard deviation. The target image's mean colour is then copied to the source image. Figures 4.2 and 4.3 show images before stain normalisation and after stain normalisation.

Algorithm : Reinhard Method(Source Image, Target Image)

1. Source and Target Images are read.
2. Convert the RGB image to colour space.

3. The Lab colour space is a transform of LMS cone space.
 - (a) Convert the RGB image into an independent XYZ space.
 - (b) Next, convert the image in XYZ space into LMS cone space. This helps in eliminating skew within the data by converting the data into logarithmic space.
4. After that distribution of data points in to Lab colour space needs to be transferred between images so source image takes on the properties of source images such as mean and standard deviation.
5. Calculate mean and standard deviation for each channel i.e there are 3 channels separate in Lab colour space.
 - (a) First subtract the mean from each data point of source image in Lab colour space.

$$L = L_s - \text{mean}(L_s) \quad (4.1)$$

$$a = a_s - \text{mean}(a_s) \quad (4.2)$$

$$b = b_s - \text{mean}(b_s) \quad (4.3)$$

where L,a,b denotes each channel in Lab colour space and L_s, a_s, b_s denotes the source image in each channel in Lab colour space.

- (b) Then normalize the mean using standard deviation

$$L_n = \text{std}(L_t) / \text{std}(L_s) * L \quad (4.4)$$

$$a_n = \text{std}(a_t) / \text{std}(a_s) * a \quad (4.5)$$

$$b_n = \text{std}(b_t) / \text{std}(b_s) * b \quad (4.6)$$

where L_n, a_n, b_n denotes the normalised mean and L_t, a_t, b_t denotes the target image in each channel in Lab colour space.

- (c) Next add the mean of target image to form the processed image

$$L_p = L_n + L_t \quad (4.7)$$

$$a_p = a_n + a_t \quad (4.8)$$

$$b_p = b_n + b_t \quad (4.9)$$

where L_p, a_p, b_p denotes the processed image in each channel in Lab colour space.

6. Convert Lab space back into RGB image. Thus stain normalized image is obtained.

The intensity variations of the source image are retained with this method. The performance of stain normalization is validated by using the structural similarity index metric (SSIM). SSIM is a reference based quality measure of an image and it is factored on the basis of luminance, contrast and structure. It ranges from -1 to 1 and the more it is closer to 1, the better the stain normalization performance is. All the images from the dataset are stain normalized to a target image taken from the A05 folder of MITOS ATYPIA 14 dataset. The performance of stain normalization is measured by the SSIM metric, which provide values in the ranges of 0.8-0.9 for each image. The resulting images after stain normalization still preserve the properties such as intensity variations of source images.

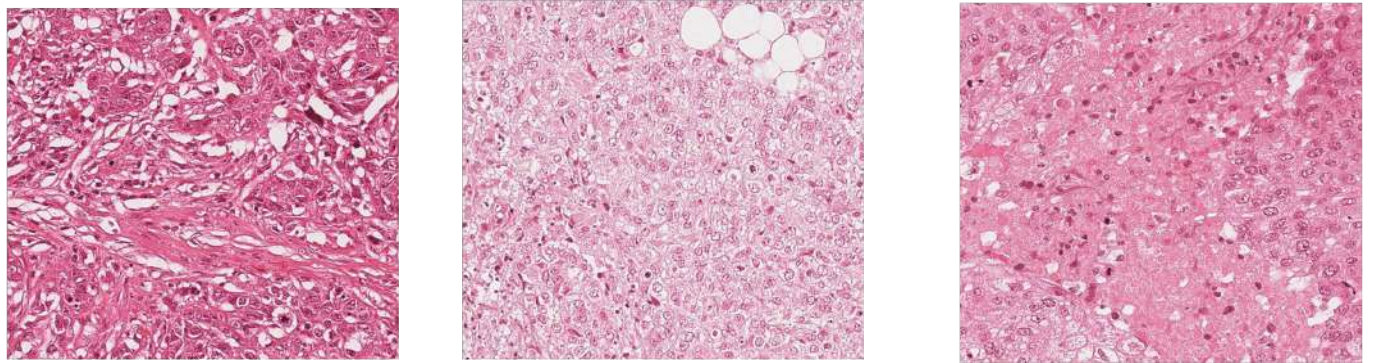


Figure 4.2: Sample images from A03,A04, A05 folders of MITOS-ATYPIA-14 dataset

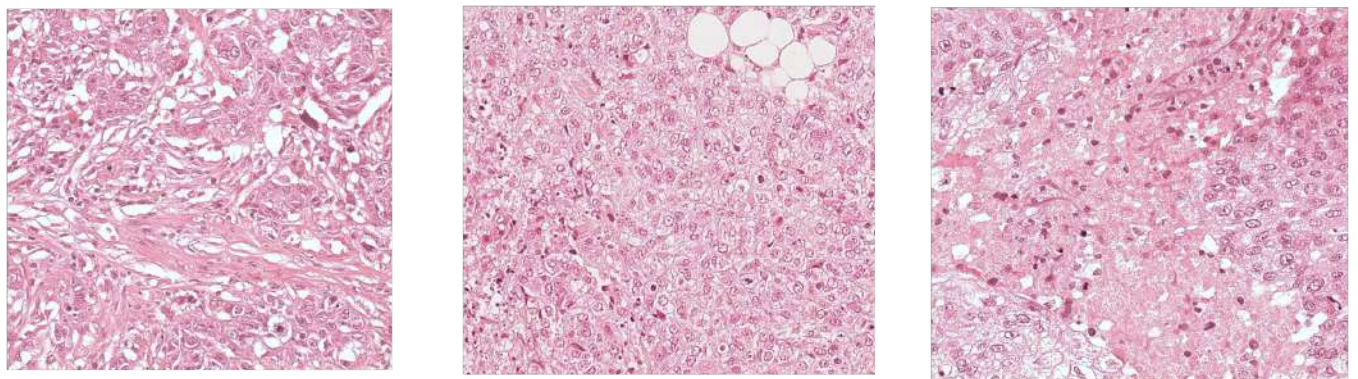


Figure 4.3: Sample images from A03,A04, A05 folders of MITOS-ATYPIA-14 dataset after stain normalisation

4.1.2 Cell segmentation and localisation

Nuclei patches of 32x32 sizes were cropped out from MITOS-ATYPIA-14 dataset and TUPAC16 dataset using its ground truths and were given as inputs to the pre-trained network models. Equal instances of both mitotic and non-mitotic cells were obtained to avoid class imbalance by augmenting few mitosis nuclei to some rotations. An equal number of mitotic and non-mitosis nuclei are included in the test set.

MITOS-ATYPIA-14 dataset

2879 instances of both mitosis and non-mitosis cells are obtained, and thus a new dataset of 5758 images of size 32x32 pixels was prepared. Equal instances of both mitotic and non-mitotic cells were obtained to avoid class imbalance by augmenting few mitosis nuclei to some rotations. An equal number of mitotic and non-mitosis nuclei are included in the test set.

TUPAC16 dataset

5282 instances of both mitosis and non-mitosis cells are obtained, and thus a new dataset of 10564 images of size 32x32 pixels was prepared. Equal instances of both mitotic and non-mitotic cells were obtained to avoid class imbalance by augmenting few mitosis nuclei to some rotations. An equal number of mitotic and non-mitosis nuclei are included in the test set.

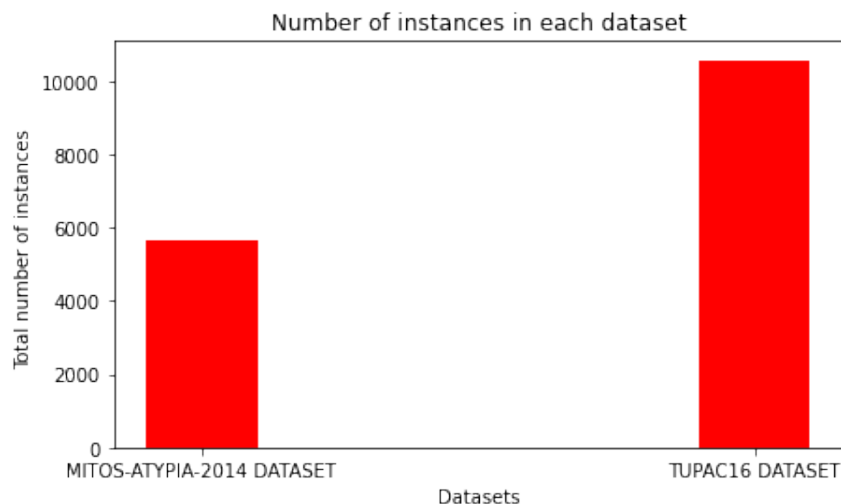


Figure 4.4: Number of instances in each dataset

4.1.3 Feature Extraction using MultiCNN framework of Pre-trained CNNs

Nuclei patches of 32x32 sizes were cropped out from MITOS-ATYPIA-14 dataset and TUPAC16 dataset were given as inputs to the pre-trained network models. We implemented a multi CNN framework consisting of pre-trained CNN models and 7 pretrained models (i.e. VGG16, Resnet-50, Densenet-201, MobileNetV2, InceptionV3, NasnetMobile and Xception) were selected for this experimental work. The networks VGG16, ResNet50, DenseNet201 already have trained weights on the ImageNet dataset. For feature extraction, several combinations of these pretrained CNNs are used. Convolution, pooling, and fully connected layers are the three layers that make up a CNN. The convolutional layer performs convolution on the input to collect distributed and correlated local information. Convolution layers perform feature extraction by convolving the input image with a set of filters. The layer typically consists of a combination of convolution operation and activation function. The convolution operation between an image I of size $i \times j$ and a filter of K size (a,b) would be

$$S_{ij} = \sum \sum I_{i-a,j-b} * K_{a,b} \quad (4.10)$$

The resulting convolved feature map is reduced along the spatial dimensions by the pooling layer. It connects all neurons in the previous layer to each neuron in the Fully-Connected Layer (FCL).

A multi CNN framework consisting of pre-trained CNN models such as VGG16, ResNet50,

DenseNet201, MobileNetV2, InceptionV3, NasnetMobile, Xception which are already trained on images of 1000 different categories was implemented. The networks already have trained weights on the ImageNet dataset. Different combinations of these pretrained CNNs are used for feature extraction. CNN typically consists of three layers: convolution, pooling, and fully connected layers. Convolution is performed by the convolutional layer to capture highly redundant and highly correlated local information in the input. The pooling layer reduces the size of the feature map along the spatial dimensions. It connects all neurons in the previous layer to each neuron in the FC layers.

VGG16

VGG16 network has a huge number of hyper-parameters, including convolution layers of filter size 3x3 with stride 1 along with same padding and a maxpool layer of 2x2 filter with stride 2. The convolution and max pooling layers follows the same arrangement throughout the architecture. The 16 in VGG16 refers to 16 layers which are assigned with different weights. the convolution layer along with the rectified linear unit that makes convolution layer. So, the number of convolution layers that in case of VGG net is 13. It has 5 max pool layers. It has got 3 fully connected unit fully connected network(FC network). So, the total number of layers having tunable parameters is 13 for convolution layer and 4 for fully connected layers, so that makes it 16, so that is why it is VGG 16. Of course, at the output you have the softmax layer having 1000 outputs, again one output per image category in the Imagenet database.

ResNet-50

ResNet-50 is a deep convolutional network which has 49 Convolution layers, 1 Max pooling layer, 1 average pooling layer, and 1 fully connected layer followed by a softmax layer for output. First layer has 64 filters of size 7x7 and stride of 2 and padding=3. Stride helps in reducing the size without using including pooling layers. It consists of batch normalization layer and max pool layer with window size 3x3 and stride of 2. Then it consists 48 layers of different filter size and filter numbers. Skip connections are provided in between – It can be plane line connections or dotted line connections. Last layer is the fully connected layer and softmax layer. Skip connections helps in solving the problem of vanishing gradient problem which is when the network tends to go to deep, the more abstract features are obtained but accuracy decreases. Skip connections skips the training from a few layers and connects directly to the output.

Densenet-201

DenseNet-201 is a variant of DenseNet architecture. Each DenseNet layer receives its input from the layers above it and passes down its feature-maps to the layers below it. Concatenation is done to combine the data from previous layers. Thus after concatenation, the network becomes more compact resulting in fewer channels. The architecture consists of 1x1 convolutional layers followed by 2x2 average pooling serve as transition layers between two contiguous dense blocks.

MobileNetV2

MobileNetV2 are a class of low power low latency models that can be used for image classification and detection. The size of MobileNet is 17 MB so these models are considered great for mobile devices, hence the name MobileNet. MobileNetV2 are tailored for resource constrained environment. MobileNetV2 contains three blocks which separates it from other CNN models. The operation of depthwise Separable Convolution is that it divides into two phases. In the depth wise, filters are applied to all channels. In the point wise, 1x1 filters are applied to all channels of outputs of previous phases. Linear Bottleneck is realised by the use of pointwise convolution and linear activation were used to reduce loss of information. Inverted Residual Block adds an expansion layer at the beginning of block and uses ReLu to add non-linearity. The inputs and output together and use the summary of them as the output of the whole block to obtain better propagation of gradients.

InceptionV3

The fundamental idea of Inception network is the inception block. In traditional CNNs, the output from the previous layer is taken and becomes the input of the next layer and it follows all upto predictions. Inception block takes up apart the individual layers and instead of passing it to one layer, it takes the previous layer input and passes it to four different operations in parallel and concatenates the outputs from all these layers. Inception V3 has 48 layers and it is trained on Imagenet dataset for 1000 classes. There are essentially 3 inception blocks with first block replaced 5x5 convolution with two 3x3 convolution layers and the third inception block replaces 3x3 convolution with asymmetric convolutions of 3x1 and 1x3 convolution. Inception V3 employs factorisation of 7x7 convolutions into asymmetric convolutions of 1x7 and 7x1 convolution in the second inception block. Each inception block ends with concatenation of features.

NasnetMobile

NasNet is introduced by Google which proposed to search the best CNN as a reinforcement learning problem. It searches the best parameters of given search space of filter sizes, output channels, strides, number of layers. The reward for each action was set by considering the accuracy of the architectural building block on the given dataset.

Xception

Xception is an efficient architecture which contains two main blocks :

1. Depthwise Separable Convolution: The filters are applied to all channels. It differs from MobileNet by that it has point wise convolution prior to depthwise separable convolution.
2. Shortcuts between Convolution blocks as in ResNet

4.1.4 Concatenation of features to form multiCNN

The feature matrix produced from each pretrained network is concatenated, The features were extracted from from each pre-trained network and are concatenated to form a feature

matrix. The sizes of images in the dataset were modified to 224x224 to match the input size for each pre-trained network. Each network acts as a feature extractor which is then concatenated to form a feature matrix of multiCNN.

4.1.5 Feature Reduction

The feature matrix produced from each pre-trained network is concatenated and then Principal Component Analysis (PCA) is employed to reduce the dimensions of these feature vectors. PCA is a technique that can be used to reduce dimensionality. The goal of PCA is to maintain maximum information of high dimensional data. High dimensional data is defined using fewer components of low dimensional subspace. Different feature matrices obtained from concatenating features of different combinations of pre-trained CNNs are passed through PCA. The data variance is set in the range of 0.95.

4.1.6 Classification of cells

The reduced feature matrix is passed to different classifiers such as LinearSVC, Non-linear SVC, Naive Bayes, Random Forest, Adaboost and XGBoost Classifier for mitosis classification.

LinearSVC and non-linear SVC

Support Vector Machines are used to solve classification and regression problems. It works by creating a hyperplane which divides the data into separate classes. LinearSVC is implemented in liblinear and it separates the data using a line into separate classes. Non-linear SVM was also employed with non-linear kernel (RBF) so it can transform the data into different dimensions and thus dividing the data into separate classes.

Logistic Regression

Logistic Regression works on the basis of probability. It is a supervised learning classification method which is used to predict the probability of the output variable. The output variable should be binary in nature. It structures a relationship between predictors and output binary variable.

Naive Bayes

Based on the Bayes theorem, the probabilistic machine learning algorithm known as Naive Bayes is used for many classification functions. The default Naive Bayes algorithm used here is Gaussian Naive Bayes.

Random Forest Classifier

Overfitting is prevented by using random forests, which are built from smaller data sets and produce results based on average or majority ranking. The data set is randomly sampled by bagging. As a result, each model is created using the samples that the original data provided, with a replacement process known as row sampling. Bootstrap refers to this stage of row sampling with replacement. Each model is currently trained independently, producing

results. After combining the outputs of all the models, the final decision is made based on a majority vote. Aggregation is the process of combining all the results and producing a result based on a majority vote.

Adaboost Classifier

A number of decision stumps are used to produce Adaboost, another ensemble learning algorithm. One node and two leaves on a decision tree are known as a decision stump. AdaBoost algorithm makes decisions by using a variety of decision stumps. After that, the tree is adjusted repeatedly to concentrate on the areas where it makes bad predictions. Because of this, Adaboost often makes predictions that are more precise than Random Forest. Adaboost, however, is also more vulnerable to overfitting than Random Forest. By building sequential models, it transforms poor learners into strong ones, with the final model having the best accuracy.

XGBoost Classifier

One common approach for boosting is gradient boosting. Each prediction corrects the mistake of its predecessor in gradient boosting. As opposed to Adaboost, each predictor is trained using the predecessor's residual errors as labels rather than adjusting the weights of the training cases. Decision trees are generated using this approach in a sequential fashion. When using XGBoost, weights are crucial. All independent variables are given weights, and the decision tree that forecasts outcomes uses these weights to predict the outcomes. The second decision tree then receives the variables that the first decision tree incorrectly anticipated and gives them more weight. They then combine these distinct classifiers and predictions to provide

4.1.7 Training

The proposed method is tested on both MITOS-ATYPIA-14 and TUPAC16 dataset. Equal instances of both mitotic and non-mitotic cells were obtained to avoid class imbalance by augmenting few mitosis nuclei to some rotations. An equal number of mitotic and non-mitosis nuclei are included in the test set. Depending on the number of outputs for the new problem, the fully-connected layer at the top of the network has been eliminated and a new fully-connected layer with one output node is introduced. The network is retrained using the new dataset, for two classes, i.e., mitotic and non-mitotic cells. Intending to improve its performance, the networks were fine-tuned with a small learning rate ($lr=1e-4$), and the last fully connected layer of each pretrained network is still replaced with a 1-node sigmoid layer.

4.1.8 Hyperparameter Tuning

The performances of deep learning models are dependent on the selection of parameters and are achieved by hyper-parameter tuning. Deep neural network parameters such as learning rate and the optimizer are selected to achieve better performance. The batch size is set as 8 and is validated on 20% of the original dataset. Fine-tuning is done by removing the fully connected layers at the end of the pre-trained networks by freezing the previous

layers so their weights cannot get updated. Then, after unfreezing the rest of the network and changing the loss function to binary cross entropy, retrain the network using Adam optimizer with a minimal learning rate of 1e-4. We train each network for 20 epochs by keeping the learning rate constant throughout training. The decay of the learning rate is set as default. The extracted features from networks are concatenated and passed to a Linear SVC, Non-Linear SVC of rbf kernel, Logistic Regression, Naive Bayes Random Forest Classifier, Adaboost classifier and XGBoost Classifier for classification. Experiments were carried out with default parameter settings for each classifier.

4.1.9 Performance Measures

The suggested methodology uses Accuracy, Precision, Recall, and F-score to evaluate mitotic identification.

$$Accuracy = \frac{TP + TN}{(TP + FP + TN + FN)} \quad (4.11)$$

$$Precision = \frac{TP}{TP + FP} \quad (4.12)$$

$$Recall = \frac{TP}{TP + FN} \quad (4.13)$$

$$F - score = \frac{2 \times (Precision) \times (Recall)}{Precision + Recall} \quad (4.14)$$

where TP denotes instances of true positives, FP denotes instances of wrongly detected mitosis. FN denote instances of incorrectly detecting mitosis as non-mitosis, and TN denote instances of correctly detected non-mitosis.

4.2 Analysis of Mitosis detection as an object detection problem

Here in this analysis, the problem of mitosis detection is worked as an object detection problem. The proposed framework in this analysis was comprised of three steps such as:

1. Stain normalisation of whole images
2. Separating the images into 4 quadrants
3. Tissue level detection using Pre-trained Faster R-CNN
4. Cell Level Classification using multiCNN framework

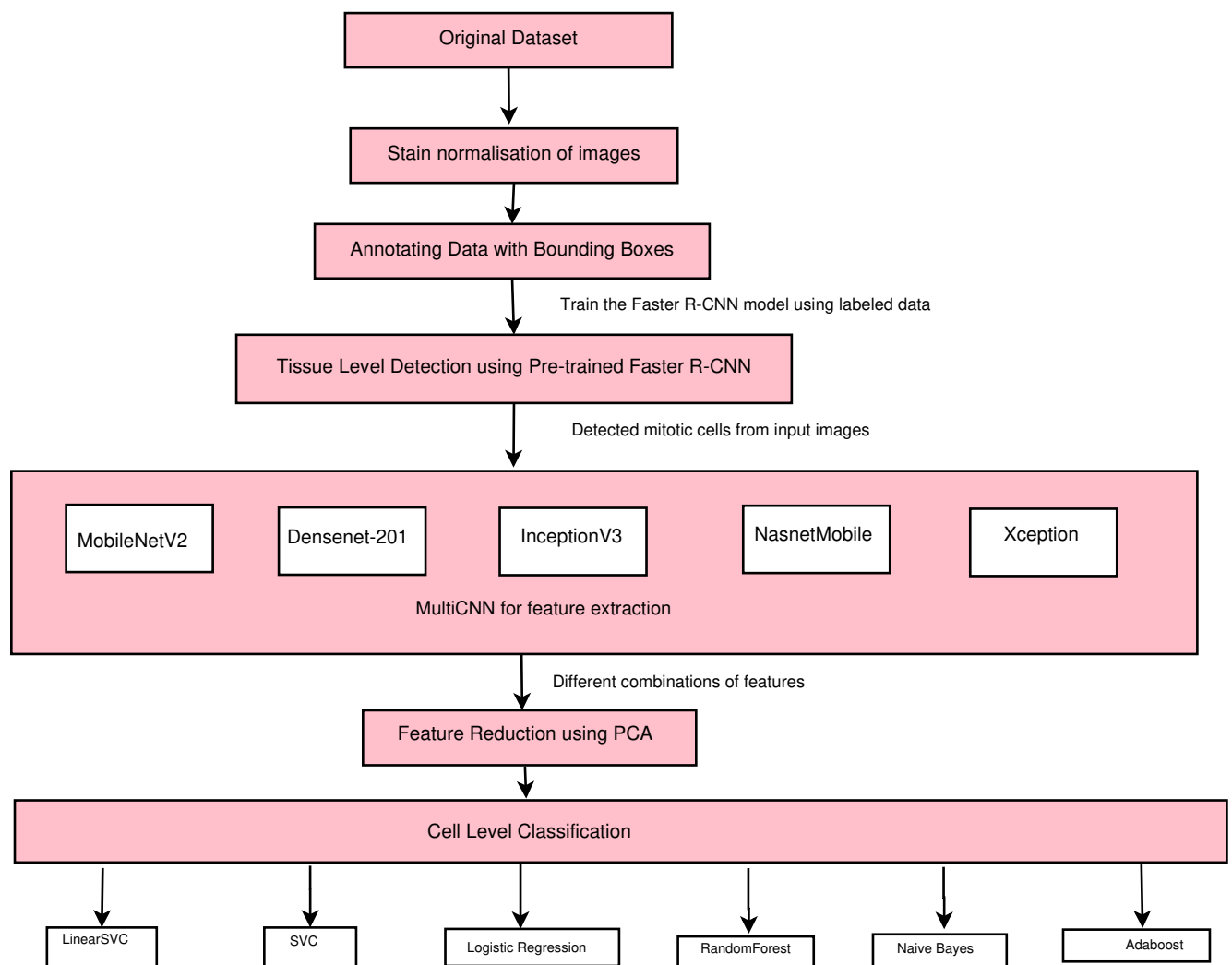


Figure 4.5: Proposed framework For Both Tissue and Cell Level Classification

4.2.1 Dataset Preparation

In this experimental analysis, the images in both MITOS-ATYPIA-2014 and TUPAC16 dataset are stain normalised.

MITOS-ATYPIA-2014 dataset

MITOS-ATYPIA-14 dataset were used for training Faster R-CNN. Images in the MITOS-ATYPIA-14 are of 1537x1376 size. Patches of size 688 x 688 were extracted from each image. Thus a single image constituted 4 patches resulting in 878 images in the training set. The labeling tool returned the labeled images along with json files which contains the coordinates of bounding box annotations and labels.

TUPAC16 dataset

TUPAC16 dataset were used as cross domain dataset to test Faster R-CNN. Images in the first 23 folders in TUPAC16 dataset are of 2000x2000 pixels and it is taken from AMIDA13 challenge. Patches of size 1000 x 1000 were extracted from each image. Thus a single image is separated into 4 quadrants as shown in Figure 4.6 resulting in the training set. The labeling tool returned the labeled images along with json files which contains the coordinates of bounding box annotations and labels. Figure 4.7 and Figure 4.8 shows how bounding boxes are drawn around ROI.

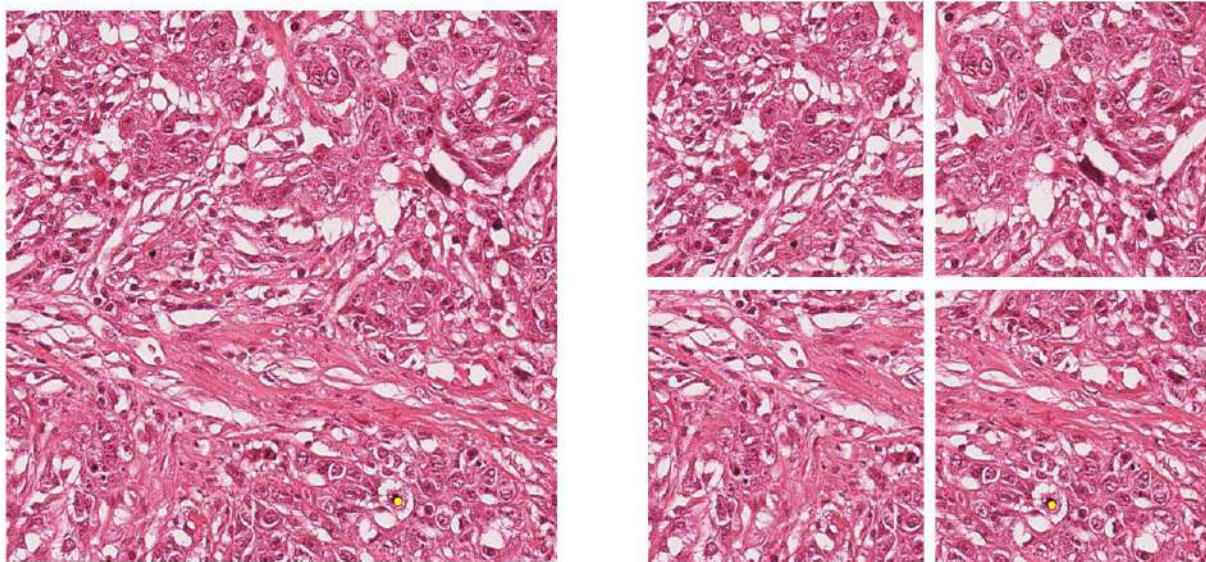


Figure 4.6: Separating the images into 4 quadrants

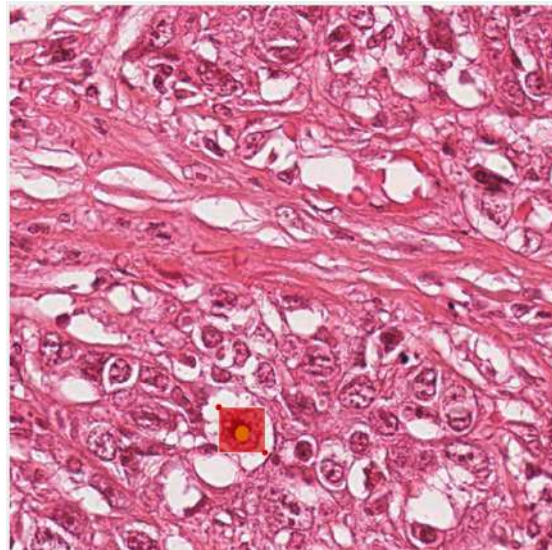


Figure 4.7: For preparation of patches as training data for object detection, bounding boxes should be drawn around ROI. Labelme tool is used for this purpose.

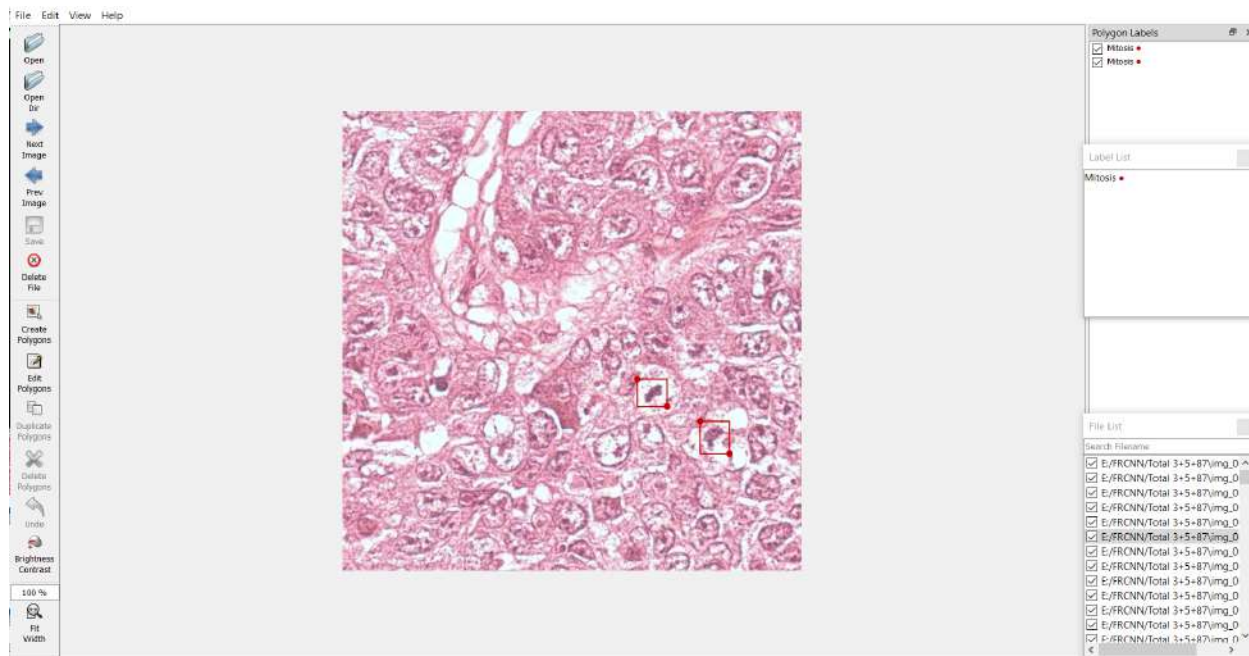


Figure 4.8: Labelme Tool for Bounding Box Preparation

4.2.2 Initial Tissue Level Detection using a pre-trained Faster R-CNN

For the initial mitotic-cell detection, the image is fed into the pretrained Faster R-CNN trained network. The Faster R-CNN is a region-based CNN that competed in the ImageNet Large-Scale Visual Recognition Challenge 2015's object-detection competition. The feature-

ANALYSIS OF MITOSIS DETECTION TECHNIQUES FOR BREAST HISTOPATHOLOGICAL IMAGES

extraction network, region proposal network (RPN), and classification network, which make up the Faster R-CNN, are a combination of three sub-networks. ResNet-50 network was used for the extraction of features for Faster R-CNN. The second part of the Faster R-CNN is the RPN. It is in charge of creating region proposals of varied sizes and ratios, which are then employed in the classification network. Anchor boxes of various scales and aspect ratios are formed over each pixel of the feature map in the RPN. Nine anchor boxes are used in general, with scales of 128, 256, and 512 and aspect ratios of 1:1, 1:2, and 2:1. The RPN predicts whether an anchor box is an object or a background. The final list of proposals is filtered using an intersection over union (IOU) threshold of 0.8 and non-maximum suppression (NMS). The feature map is cropped at a given location in the classification network using region proposals. Because each of the cropped feature maps is a different size, ROI pooling is used to achieve a consistent size. After passing through completely connected layers, the bounding box regression vectors and mitotic cell probabilities are produced. The bounding box regression vectors are used to refine proposal boxes into prediction boxes, which is then followed by the elimination of overlapping boxes by NMS to provide the final detection findings. After putting the complete Faster R-CNN model together, then train it end-to-end as a single network, with four losses, RPN classification loss, RPN regression loss, R-CNN classification loss and R-CNN regression loss.

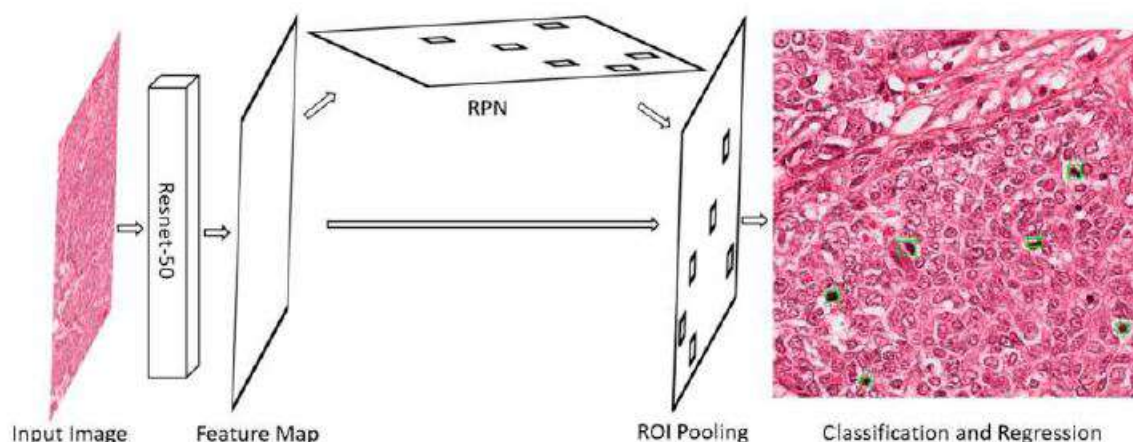


Figure 4.9: Mitosis Detection using Faster R-CNN

Pre trained Resnet 50 backed Faster R-CNN were implemented using Tensorflow 1.x Object Detection. The model was trained over 80000 iterations with batch size 8 and learning rate 0.0002 for 790 images.

The annotation files and images are to be converted to TFRecord format so Tensorflow 1.x Object Detection API can be used for detection. A TFRecord file stores the data as a sequence of binary strings. The TFRecord file act as a wrapper around all the single data samples. Every single data sample is called an Example and is essentially a dictionary storing the mapping between a key and the actual data.

The trained Faster R-CNN is then tested on a testing set which results in a large number of false positive cases. The detected patches are then cropped out and are used to train the

pre-trained multiCNN framework for feature extraction and cell level classification.

4.2.3 Cell Level Detection using MultiCNN framework

Different pre-trained CNNs constitute to form a multiCNN framework and thus feature extraction is done by extracting and combining features from each CNNs to different combinations. The detected objects from the Faster R-CNN are passed through the multiCNN framework for classification. VGG16, ResNet50, Densenet201, InceptionV3, MobileNetV2, NasnetMobile, Xception were selected as the pre-trained CNNs in this experimental analysis. The detected objects from Faster R-CNN are to be cropped out and resized to 224x224 so that the image size would be compatible with all these pre-trained CNNs trained over Imagenet database. Image augmentation techniques like vertical and horizontal flip, translation are done to increase the number of training data to train pre-trained CNNs. Each pre-trained CNNs produces a feature matrix of size $n \times m$ where n is the number of images and m is the number of features. The multiCNN is formed by the concatenation of these feature matrices, resulting in a feature matrices of $n \times bm$ where b is the number of pre-trained CNNs.

4.2.4 Feature Reduction and Classification of cells

The feature matrix produced from each pre-trained network is concatenated and then Principal Component Analysis (PCA) is employed to reduce the dimensions of these feature vectors. PCA is a technique that can be used to reduce dimensionality. The goal of PCA is to maintain maximum information of high dimensional data. High dimensional data is defined using fewer components of low dimensional subspace. Different feature matrices obtained from concatenating features of different combinations of pre-trained CNNs are passed through PCA. The data variance is set in the range of 0.95. The reduced feature matrix is passed to different classifiers such as LinearSVC, Non-linearSVC, Logistic Regression, Naive Bayes, Random Forest, Adaboost, XGBoost for mitosis classification.

4.2.5 Performance Measures

The suggested methodology uses Accuracy, Precision, Recall, and F-score to evaluate mitotic identification.

$$Accuracy = \frac{TP + TN}{(TP + FP + TN + FN)} \quad (4.15)$$

$$Precision = \frac{TP}{TP + FP} \quad (4.16)$$

$$Recall = \frac{TP}{TP + FN} \quad (4.17)$$

$$F - score = \frac{2 \times (Precision) \times (Recall)}{Precision + Recall} \quad (4.18)$$

where TP denotes instances of true positives, FP denotes instances of wrongly detected mitosis. FN denote instances of incorrectly detecting mitosis as non-mitosis, and TN denote instances of correctly detected non-mitosis.

Chapter 5

Results and Discussions

5.1 Analysis of Mitosis detection as a classification problem

5.1.1 Datasets considered

MITOS-ATYPIA-14 dataset had 2828 instances of mitotic and non-mitotic cells each and it was split into 70% as training set and 30% for testing set. Another cross domain dataset, TUPAC16 dataset which had 5282 instances of mitotic and non-mitotic cells after image augmentation are also tested. The method is tested on both datasets.

5.1.2 Performance comparison of dimensionality reduction methods

The concatenated features of different pre-trained networks are passed through different dimensionality reduction methods such as PCA, Truncated SVD, Gaussian Random Projection before coupling with a classifier. The experiment showed that the multiCNN of 6 pre-trained CNNs gave better accuracy, precision, F-score and recall when PCA is adopted as dimensionality reduction method coupled with non-Linear SVC as classifier.

Feature Reduction	Accuracy	Precision	F-score	Recall
PCA	0.907	0.942	0.904	0.869
Truncated SVD	0.895	0.933	0.890	0.852
Gaussian Random Projection	0.886	0.916	0.882	0.852

Table 5.1: Comparison of results obtained for multiCNN of 6 pre-trained CNNs using different dimensionality reduction methods with non-linear SVC as classifier

5.1.3 Performance comparison of multiCNN composed of 6 pre-trained CNNs with different classifiers

The multiCNN composed of 6 pre-trained CNNs (Densenet-201, MobileNetV2, InceptionV3, NasnetMobile, Xception, VGG16) which gave the best performance with non-linear SVC as classifier were compared with other classifiers. All other classifiers could not obtain a comparable performance with non-linear SVC. Naive Bayes and Random Forest gave poor

performance when coupled with multiCNN of 6 pre-trained CNNs and it showed similar performance when coupled with different pre-trained networks.

Model	Accuracy	Precision	F-score	Recall
LinearSVC	0.881	0.903	0.878	0.854
Logistic Regression	0.883	0.898	0.882	0.866
Naive Bayes	0.652	0.636	0.673	0.714
Adaboost	0.817	0.820	0.815	0.815
RandomForest	0.759	0.798	0.744	0.696
XGBoost	0.853	0.883	0.848	0.815

Table 5.2: Comparison of results obtained for multiCNN of 6 pre-trained CNNs using different classifiers

5.1.4 Results of pre-trained multi-CNN with different combinations of networks on MITOS-ATYPIA-14 dataset

Experimental analysis were conducted on the concatenated features obtained from different pre-trained networks. The results of different combinations of pre-trained CNNs with Non-Linear SVC as classifier which were tested on MITOS-ATYPIA-14 dataset are shown in Table 5.3. The networks are then fine-tuned with a small learning rate ($lr=1e-4$) and it is done by removing the fully connected layers at the end of the pre-trained networks by freezing the previous layers so their weights cannot get updated. 7 pre-trained CNNs were taken for this experimental analysis.

It can be observed that multiCNN architecture of pre-trained CNNs gave better results than that of a single one. It can be observed that multiCNN architecture of pre-trained CNNs gave better results than that of a single one. The best performing single CNNs were combined to observe its performance. And the combination of 6 pre-trained CNNs (VGG16, InceptionV3, MobileNetV2, Densenet-201, NasnetMobile, Xception) resulted in an accuracy of 0.907 and precision of 0.942 which were far better results compared to multi-CNNs of 4 and 5 pre-trained CNNs. The confusion matrix and ROC curve corresponding to multiCNN of 6 pre-trained CNNs applied on TUPAC16 dataset are shown in Table 5.4 and Figure 5.1 respectively.

ANALYSIS OF MITOSIS DETECTION TECHNIQUES FOR BREAST
HISTOPATHOLOGICAL IMAGES

MultiCNN model used for feature extraction	Feature Reduc- tion	Accuracy	Precision	F-score	Recall
Densenet-201+NasnetMobile + Mo- bileNetV2+ InceptionV3 +Xcep- tion+VGG16	PCA	0.907	0.942	0.904	0.869
Densenet-201+NasnetMobile+MobileNetV2 +InceptionV3 +Xception		0.902	0.935	0.899	0.866
Densenet-201+NasnetMobile+MobileNetV2+ InceptionV3		0.900	0.930	0.898	0.866
Densenet-201+NasnetMobile+MobileNetV2 +Xception		0.906	0.941	0.903	0.868
NasnetMobile+MobileNetV2+InceptionV3 +Xception		0.897	0.929	0.893	0.860
Densenet-201+ NasnetMobile+ InceptionV3		0.906	0.936	0.903	0.871
Densenet-201+ NasnetMobile + Xception		0.906	0.933	0.904	0.875
Densenet-201+MobileNetV2+InceptionV3		0.899	0.929	0.896	0.865
Densenet-201+MobileNetV2+Xception		0.898	0.933	0.895	0.861
Densenet-201+ InceptionV3+Xception		0.901	0.927	0.899	0.872
NasnetMobile+MobileNetV2 +Xception		0.898	0.933	0.895	0.861
NasnetMobile+ InceptionV3+Xception		0.907	0.937	0.904	0.873
NasnetMobile+MobileNetV2+InceptionV3		0.902	0.931	0.898	0.868
Densenet-201+ +InceptionV3		0.889	0.931	0.896	0.862
Densenet-201+ Xception		0.905	0.934	0.901	0.873
MobileNetV2 +Xception		0.87	0.907	0.876	0.847
InceptionV3+Xception		0.885	0.905	0.882	0.861
MobileNetV2+InceptionV3		0.883	0.903	0.881	0.860
NasnetMobile+MobileNetV2		0.89	0.919	0.886	0.856
NasnetMobile+Xception		0.875	0.895	0.873	0.852
MobileNetV2	0.861	0.877	0.859	0.814	
InceptionV3	0.861	0.882	0.857	0.835	
VGG16	0.850	0.901	0.841	0.788	
NasnetMobile	0.855	0.871	0.852	0.833	
Xception	0.857	0.874	0.854	0.833	

Table 5.3: Results of various multiCNN modelwith Non-Linear SVC as classifier

		Predicted Values	
		Mitosis	Non Mitosis
Actual values	Mitosis	754.0	113.0
	Non-Mitosis	47.0	814.0

Table 5.4: Confusion matrix corresponding to multiCNN of 6 pre-trained CNNs coupled with non-linear SVC on MITOS-ATYPIA-14 dataset

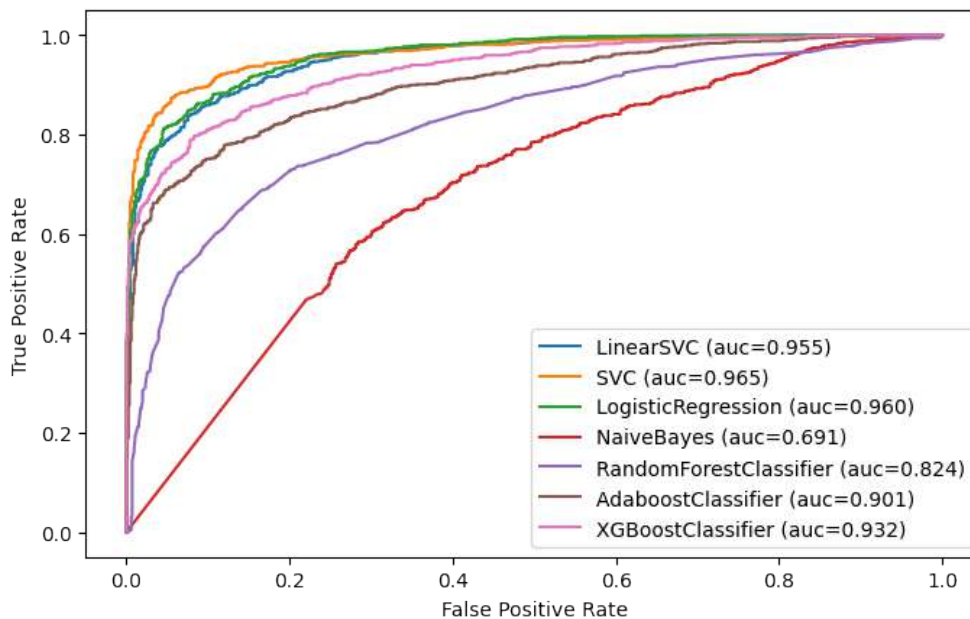


Figure 5.1: ROC curve corresponding to multiCNN of 6 pre-trained CNNs' results obtained in MITOS-ATYPIA-14 dataset

5.1.5 Classification Results obtained on TUPAC16 dataset

The multiCNN framework is applied on TUPAC16 dataset which were split into 70% of training set and 30% testing set. The results of different combinations of pre-trained CNNs with Non-Linear SVC as classifier which were tested on TUPAC16 dataset are shown in Table 5.5. The confusion matrix and ROC curve corresponding to multiCNN of 6 pre-trained CNNs applied on TUPAC16 dataset are shown in Table 5.6 and Figure 5.2 respectively.

MultiCNN model for feature extraction	Accuracy	Precision	F-score	Recall
Densenet-201 + NasnetMobile + MobileNetV2 +InceptionV3 +Xception+VGG16	0.92	0.955	0.916	0.881
Densenet-201+NasnetMobile+MobileNetV2 +InceptionV3 +Xception	0.9186	0.9529	0.9155	0.8809
Densenet-201+NasnetMobile+MobileNetV2+ InceptionV3	0.9182	0.9547	0.9149	0.8783
Densenet-201+NasnetMobile+MobileNetV2 +Xception	0.906	0.941	0.903	0.868
NasnetMobile+MobileNetV2+InceptionV3 +Xception	0.905	0.933	0.9019	0.8727
Densenet-201+ NasnetMobile+ InceptionV3	0.917	0.95	0.914	0.8809
Densenet-201+ NasnetMobile + Xception	0.906	0.933	0.904	0.875
Densenet-201+MobileNetV2+InceptionV3	0.918	0.951	0.915	0.8809
Densenet-201+MobileNetV2+Xception	0.919	0.953	0.916	0.8809
Densenet-201+ InceptionV3+Xception	0.916	0.948	0.913	0.88
NasnetMobile+MobileNetV2 +Xception	0.898	0.933	0.895	0.861
NasnetMobile+ InceptionV3+Xception	0.901	0.925	0.898	0.872
NasnetMobile+MobileNetV2+InceptionV3	0.902	0.931	0.898	0.868
Densenet-201+ +InceptionV3	0.916	0.947	0.913	0.88
Densenet-201+ Xception	0.918	0.953	0.915	0.88
MobileNetV2 +Xception	0.89	0.924	0.883	0.855
InceptionV3+Xception	0.88	0.906	0.88	0.857
MobileNetV2+InceptionV3	0.892	0.913	0.889	0.867
NasnetMobile+MobileNetV2	0.897	0.925	0.894	0.865
NasnetMobile+Xception	0.882	0.904	0.878	0.856
InceptionV3	0.861	0.882	0.857	0.835
Xception	0.857	0.874	0.854	0.839
NasnetMobile	0.855	0.871	0.852	0.833

Table 5.5: Results of concatenation of features from different pre-trained networks with Non-Linear SVC as classifier

		Predicted Values	
		Mitosis	Non Mitosis
Actual values	Mitosis	1398.0	189.0
	Non-Mitosis	66.0	1517.0

Table 5.6: Confusion matrix corresponding to multiCNN of 6 pre-trained CNNs coupled with non-linear SVC

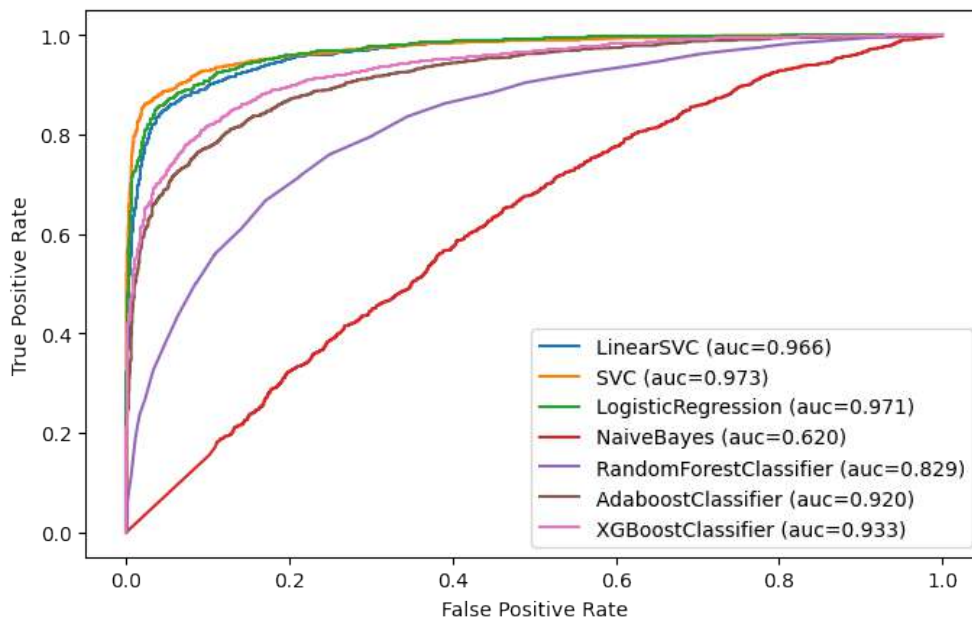


Figure 5.2: ROC curve corresponding to multiCNN of 6 pre-trained CNNs' results obtained in TUPAC16 dataset

5.1.6 Results of proposed method with the other methodologies in the literature

The proposed method is compared against other works as shown in Table 5.7.

Technique	Model	Dataset	Precision	F-score	Recall
Zerhouni et.al[7]	Wide Residual Network	TUPAC16	0.675	0.648	0.623
H.Chen et.al [8]	Deep cascaded networks	MITOS-ATYPIA-14	0.460	0.482	0.507
H. Wahab et. al. [17]	Pre-trained CNN+Hybrid CNN	TUPAC16	0.772	0.714	0.663
Proposed method	MultiCNN	MITOS-ATYPIA-14	0.942	0.904	0.869
	MultiCNN	TUPAC16	0.955	0.916	0.881

Table 5.7: Results of different deep learning based mitosis detection methods with proposed method

5.2 Analysis of mitosis detection as an object detection problem

5.2.1 Detection of patches from the test images using Faster R-CNN

The detected objects from Faster R-CNN have different confidence scores of which the arbitrary set threshold, say, 0.7 were chosen so as to crop out good candidate regions. Figures 5.3 and 5.4 show detected objects using Faster R-CNN and detected objects cropped out from testing data.

5.2.2 Performance comparison of multiCNN architecture with a single pre-trained CNN on MITOS-ATYPIA-14 dataset

Experimental analysis were conducted on the concatenated features obtained from different pre-trained networks. The results of different combinations of pre-trained CNNs with Logistic Regression as classifier which were tested on detected images of MITOS-ATYPIA-14 dataset are shown in Table 5.8.

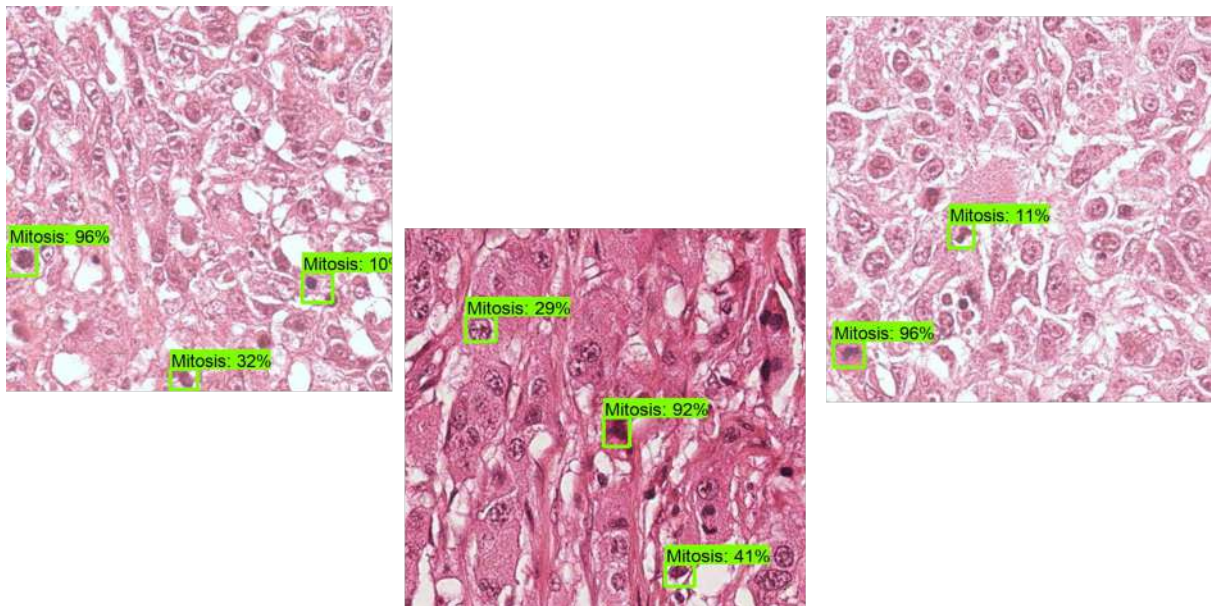


Figure 5.3: Mitosis Detection using Faster R-CNN

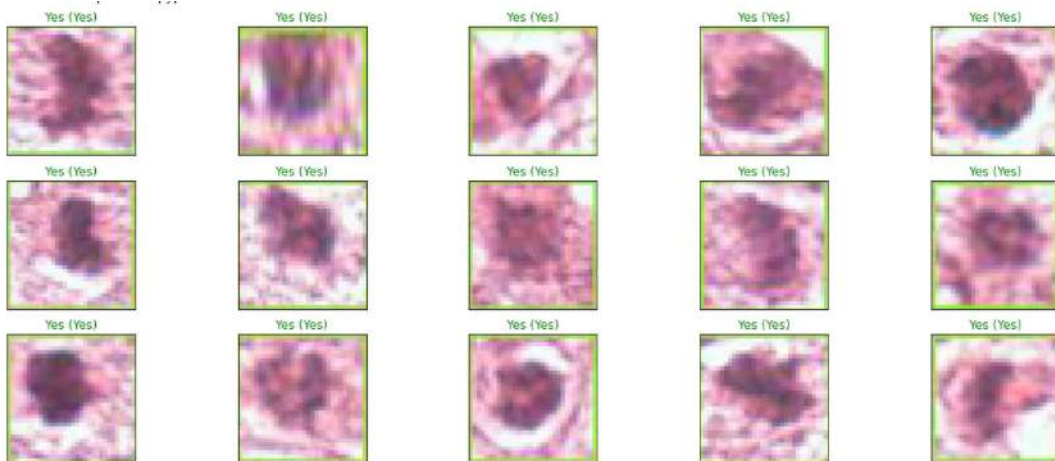


Figure 5.4: Detected objects which are cropped out from testing data

ANALYSIS OF MITOSIS DETECTION TECHNIQUES FOR BREAST HISTOPATHOLOGICAL IMAGES

MultiCNN	Accuracy	Precision	F-score	Recall
Densenet-201+NasnetMobile+ MobileNetV2 + InceptionV3 + Xception	0.92	0.922	0.922	0.922
Densenet-201+VGG16+MobileNetV2 +InceptionV3+Xception	0.916	0.915	0.918	0.922
Densenet-201+MobileNetV2+InceptionV3 +VGG16	0.888	0.898	0.891	0.884
Densenet-201+NasnetMobile+MobileNetV2+ InceptionV3	0.896	0.905	0.898	0.891
Densenet-201+NasnetMobile+MobileNetV2 +Xception	0.916	0.905	0.898	0.892
Densenet-201+NasnetMobile+InceptionV3 +Xception	0.908	0.907	0.911	0.915
Densenet-201+NasnetMobile+InceptionV3 +Xception	0.908	0.907	0.911	0.915
NasnetMobile+MobileNetV2+InceptionV3 +Xception	0.888	0.891	0.891	0.891
Densenet-201+MobileNetV2+InceptionV3 +Xception	0.904	0.907	0.907	0.907
Densenet-201+ NasnetMobile+MobileNetV2	0.888	0.924	0.887	0.852
Densenet-201+ NasnetMobile+ InceptionV3	0.912	0.915	0.915	0.915
Densenet-201+ NasnetMobile + Xception	0.888	0.910	0.888	0.868
Densenet-201+MobileNetV2+InceptionV3	0.912	0.928	0.913	0.899
Densenet-201+MobileNetV2+Xception	0.904	0.901	0.907	0.914
Densenet-201+ InceptionV3+Xception	0.864	0.874	0.867	0.860
NasnetMobile+MobileNetV2 +Xception	0.876	0.901	0.876	0.853
NasnetMobile+ InceptionV3+Xception	0.9	0.912	0.902	0.891
NasnetMobile+MobileNetV2+InceptionV3	0.892	0.898	0.895	0.891
Densenet-201+ NasnetMobile	0.912	0.921	0.914	0.907
Densenet-201+ +InceptionV3	0.88	0.896	0.882	0.868
Densenet-201+ Xception	0.892	0.904	0.894	0.884
Densenet-201+ MobileNetV2	0.864	0.874	0.867	0.861
MobileNetV2 +Xception	0.888	0.904	0.89	0.876
InceptionV3+Xception	0.916	0.92	0.918	0.915
MobileNetV2+InceptionV3	0.852	0.859	0.856	0.853
NasnetMobile+MobileNetV2	0.836	0.867	0.835	0.806
NasnetMobile+Xception	0.864	0.875	0.872	0.868
Densenet-201	0.884	0.884	0.888	0.891
Resnet50	0.728	0.736	0.736	0.736
MobileNetV2	0.828	0.846	0.830	0.814
InceptionV3	0.868	0.875	0.872	0.868
VGG16	0.804	0.807	0.811	0.814
NasnetMobile	0.816	0.826	0.820	0.814
Xception	0.816	0.837	0.817	0.798

Table 5.8: Results of concatenation of features from different pre-trained networks with Logistic Regression as classifier

It can be observed that multiCNN architecture of pre-trained CNNs gave better results than that of a single one. The best performing single CNNs were primarily used to form multiCNN architecture with 2 multiCNNs composed of 5 pre-trained CNNs and 4 multiCNNs composed of 4 pre-trained CNNs obtained accuracy of more than 90%. The best performance were observed in the multiCNN composed of 5 pre-trained CNNs (i.e Densenet-201, NasnetMobile, MobileNetV2, InceptionV3, Xception). It gave an accuracy of 92% and F-score of 92.2%.

5.2.3 Performance comparison of multiCNN composed of 5 pre-trained CNNs with different classifiers

The multiCNN composed of 5 pre-trained CNNs (Densenet-201, MobileNetV2, InceptionV3, NasnetMobile, Xception) which gave the best performance with Logistic Regression were compared with other classifiers in Table 5.9. Of which, non-linear SVC of rbf kernel gave comparable performance with performance metrics above 90%. The ROC curve corresponding to results obtained after cell level classification is shown in Figure 5.5.

Model	Accuracy	Precision	F-score	Recall
LinearSVC	0.896	0.9055	0.898	0.8914
SVC(rbf kernel)	0.912	0.922	0.914	0.907
Naive Bayes	0.78	0.731	0.809	0.907
Adaboost	0.832	0.837	0.837	0.837
RandomForest	0.81	0.739	0.898	0.90

Table 5.9: Comparison of results obtained for multiCNN of 5 pre-trained CNNs using different classifiers

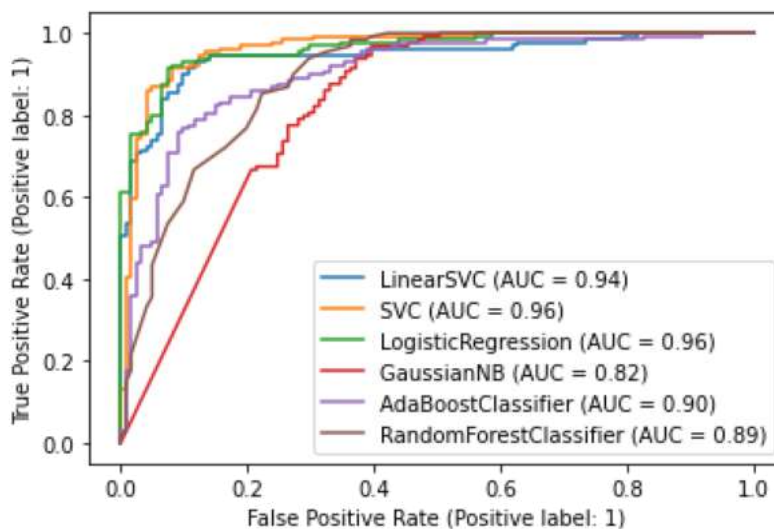


Figure 5.5: ROC curve corresponding to results obtained after cell level classification

Chapter 6

Conclusion

The problem of mitosis detection was analysed as a classification and an object detection problem in this work. First, the problem of mitosis detection is analysed as a classification problem by proposing a multiCNN framework for feature extraction and classifying it using other classifiers. First, the dataset is passed into each pre-trained network, and the performance metrics of each pre-trained network after further fine-tuning are measured. Features are then extracted from these pre-trained networks and concatenated into different feature matrices. These feature matrices are fed to Principal Component Analysis where the dimensionality of these features is reduced. Then the images with reduced features are passed to LinearSVC, Non-linear SVC, Logistic Regression, Naive Bayes, Random Forest Classifier, Adaboost classifier and XGBoost Classifier to classify mitotic cells. Performance metrics are also measured. MultiCNN of 6 fine-tuned pre-trained CNNs (VGG16, Densenet201, InceptionV3, MobileNetV2, NasnetMobile, Xception) with non - LinearSVC as classifier gave overall better accuracy and precision than all other combinations of multi-CNN architectures with other classifiers for MITOS-ATYPIA-14 dataset. The same multi-CNN also gave a better accuracy and recall when it was applied to TUPAC16 dataset. The proposed method performs classification between mitotic and non-mitotic cells only. This experimental analysis only worked with 7 pre-trained CNNs and different pre-trained CNNs can be used as multiCNN feature extractors to extend this work.

Then the problem of mitosis detection is tackled as an object detection problem. The analysis is done on MITOS-ATYPIA 2014 dataset and TUPAC16 dataset. Patches were extracted from stain normalised images as inputs to pre-trained Faster-RCNN. The detected boxes on the test images obtained from Faster R-CNN were cropped out for a final classification using deep CNNs. The cell level classification is done by extracting and concatenating features from each model and feeding it to different classifiers. Resnet-50 backed Faster R-CNN was primarily trained on MITOS-ATYPIA-14 dataset and the cell level classification of test images from MITOS-ATYPIA-14 dataset using multiCNN of 5 pre-trained CNNs resulted in an AUC of 0.96, Precision of 92.2%. The cell level classification of detected patches of TUPAC16 dataset showed less performance. This can be improved if the Faster R-CNN model is trained on TUPAC16 dataset and can be extended as future work.

References

- [1] Tashk A, Helfroush M, Danyali H, Akbarzadeh-Jahromi M. An automatic mitosis detection method for breast cancer histopathology slide images based on objective and pixel-wise textural features classification. In The 5th Conference on Information and Knowledge Technology 2013, p. 406–10.
- [2] Irshad H, Jalali S, Roux L, Racoceanu D, Hwee L, Le Naour G, et al. Automated mitosis detection using texture, sift features and hmax biologically inspired approach. *Journal of Pathology Informatics* Mar 2013;4:S12
- [3] Paul A, Mukherjee D. Mitosis detection for invasive breast cancer grading in histopathological images. *IEEE Transactions on Image Processing* 2015 Jul 23;24(11):p-4041-4054.
- [4] Khan A, Eldaly H, Rajpoot N. A gamma-gaussian mixture model for detection of mitotic cells in breast cancer histopathology images. *Journal of Pathology Informatics*. Jan-Dec 2013;4(1):11
- [5] Tek F. Mitosis detection using generic features and an ensemble of cascade adaboosts. *Journal of Pathology Informatics*.Jan–Dec 2013;4(2):12.
- [6] Cireşan DC, Giusti A, Gambardella LM, Schmidhuber J. Mitosis detection in breast cancer histology images with deep neural networks. In *International conference on medical image computing and computer-assisted intervention* 2013 Sep 22 (pp. 411-418). Springer, Berlin, Heidelberg.
- [7] Zerhouni E, Lányi D, Viana M, Gabrani M. Wide residual networks for mitosis detection. In *2017 IEEE 14th International Symposium on Biomedical Imaging (ISBI 2017)* 2017 Apr 18 (pp. 924-928). IEEE.
- [8] Chen H, Dou Q, Wang X, Qin J, Heng PA. Mitosis detection in breast cancer histology images via deep cascaded networks. In *Thirtieth AAAI conference on artificial intelligence* 2016 Feb 21 (pp 1160-1166).
- [9] Beevi KS, Nair MS, Bindu GR. A multi-classifier system for automatic mitosis detection in breast histopathology images using deep belief networks. *IEEE Journal of Translational Engineering in Health and Medicine*. 2017 Apr 25;5:1-1.
- [10] Cai D, Sun X, Zhou N, Han X, Yao J. Efficient mitosis detection in breast cancer histology images by RCNN.In *2019 IEEE 16th International Symposium on Biomedical Imaging (ISBI 2019)*.2019 Jul 11, p. 919–22.

- [11] Mahmood T, Arsalan M, Owais M, Lee MB, Park KR. Artificial intelligence-based mitosis detection in breast cancer histopathology images using faster R-CNN and deep CNNs. *Journal of clinical medicine*. 2020 Mar;9(3):749.
- [12] Sebai M, Wang T, Ali S. Partmitosis: A partially supervised deep learning framework for mitosis detection in breast cancer histopathology images. *IEEE Access* 2020.2020 Mar 5;8:45133 - 45147.
- [13] Sebai M, Wang X, Wang T. MaskMitosis: a deep learning framework for fully supervised, weakly supervised, and unsupervised mitosis detection in histopathology images. *Medical Biological Engineering Computing*. 2020 Jul;58:1603-23.
- [14] Lei H, Liu S, Xie H, Kuo JY, Lei B. An improved object detection method for mitosis detection. In 2019 41st Annual International Conference of the IEEE Engineering in Medicine and Biology Society (EMBC) 2019 Jul 23 (pp. 130-133). IEEE.
- [15] Beevi KS, Nair MS, Bindu GR. Automatic mitosis detection in breast histopathology images using Convolutional Neural Network based deep transfer learning. *Biocybernetics and Biomedical Engineering*. 2019 Jan 1;39(1):214-23.
- [16] Dodballapur V, Song Y, Huang H, Chen M, Chrzanowski W, Cai W. Mask-driven mitosis detection in histopathology images. In 2019 IEEE 16th International Symposium on Biomedical Imaging (ISBI 2019).p. 1855 - 1859
- [17] Wahab N, Khan A, Lee YS. Transfer learning based deep CNN for segmentation and detection of mitoses in breast cancer histopathological images. *Microscopy*. 2019 Jun 1;68(3):216-33.
- [18] Abraham B, Nair M.S. Computer aided detection of covid-19 from x-ray images using MultiCNN and Bayesnet classifier. *Biocybernetics And Biomedical Engineering*.2020 Sep 02. 40(4):1436–1445,
- [19] Kausar T, Wang M, Ashraf MA, Kausar A. SmallMitosis: Small Size Mitotic Cells Detection in Breast Histopathology Images. *IEEE Access*. 2020 Dec 14;9:905-22.
- [20] Sohail A, Khan A, Wahab N, Zameer A, Khan S. A multi-phase deep CNN based mitosis detection framework for breast cancer histopathological images. *Scientific Reports*. 2021 Mar 18;11(1):1-8.
- [21] MITOS-ATYPIA-14 Grand Challenge. Available online: <https://mitos-atypia-14.grand-challenge.org/>.
- [22] TUPAC16 Grand Challenge . Available online:<https://tupac.grand-challenge.org/>.